Surface Modification of Poly(tetrafluoroethylene) by Remote Hydrogen Plasma

Y. Yamada, T. Yamada, S. Tasaka, and N. Inagaki*

Laboratory of Polymer Chemistry, Faculty of Engineering, Shizuoka University, 3-5-1 Johoku, Hamamatsu, 432 Japan

Received July 24, 1995; Revised Manuscript Received March 11, 1996[⊗]

ABSTRACT: The kinetics of hydrogen plasma in an afterglow region has been simulated to distinguish remote plasma treatment from conventional (direct) plasma treatment. A simulation shows the possibility that remote hydrogen plasma treatment can enhance interaction reactions with hydrogen radicals relative to those with electron and hydrogen ions. Practically, hydrogen substitution processes in the PTFE sheet by remote and direct hydrogen plasma treatments have been investigated by means of contact angle measurement and XPS. The hydrogen plasma makes the surface of the PTFE sheet hydrophilic. The hydrophilicity depends on the sample position as well as the rf power and the plasma exposure time. The sample position strongly influences the hydrophilicity. The remote hydrogen plasma leads to higher hydrophilicity than the direct hydrogen plasma. The F/C atom ratio for the remote hydrogen-plasma-treated PTFE sheet is 0.41 and that for the direct hydrogen-plasma-treated PTFE sheet is 0.60. The main product of the substitution atoms by remote and direct hydrogen plasma treatments is a dihydrogen-substituted carbon unit and reaches 63% and 55% of the total carbon, respectively. The substitution proceeds at least 3.4 nm from the surface of the PTFE sheet. Remote hydrogen plasma treatment especially accomplishes complete substitution (the F/C atom ratio is 0). These experimental results show the accuracy of the simulation regarding the kinetics of the remote hydrogen plasma.

1. Introduction

Fluorine-containing polymers, e.g., poly(tetrafluoroethylene), PTFE, possess good hydrophobic surfaces (the surface energy of PTFE is 18.6 mJ/m^2). The hydrophobicity is a result of the low polarizability of the C−F bonds. The hydrophobic surface of PTFE is a distinguishing property but a knotty problem in adhesion with other materials. Many investigators have studied the surface modification of PTFE by means of chemicals, graft polymerization, sputtering, and plasma treatment.[1] Substitution of hydrophilic groups such as hydroxyl and carbonyl groups for fluorine atoms is an essential reaction in the surface modification of PTFE. The initiation of the substitution reaction is not so easy because of the high bond energy of the C−F bond (486 kJ/mol) and requires highly reactive chemicals (sodium naphthalene complex) or high energy input.

Plasma contains highly activated species such as electron, ions, and radicals and can initiate chemical reactions. Schonhorn and Hansen[2] first applied plasma for the surface modification of PTFE, and succeeded in hydrophilic modification. After their success, many investigators have discussed the plasma modification, and reported new ways for using plasma for surface modification.[3−6] In chemistry, the modification may be radical reactions. If we can isolate radicals from the plasma, the radicals will react effectively with the surface of PTFE to initiate the substitution reaction of fluorine atoms in PTFE.

Plasma is a good source of radicals, although the plasma contains electrons and positive and negative ions besides radicals. These species disappear in processes of electron−positive ion recombination and atom recombination. The first process (electron−positive ion recombination) is much faster than the other (atom recombination). The rate constants of these recombination reactions are on the order of 10^{-7} cm^3/s, and 10^{-33} cm^6/s, respectively.[7] Therefore, radicals possess longer lifetimes than electrons and ions. We expect that the radical concentration at the position away from the plasma zone may be predominantly higher than the electron and ion concentrations because of the longer lifetimes of radicals.

In this study, we have focused on hydrogen plasma as a source of hydrogen radicals (hydrogen atoms), and the hydrogen substitution of fluorine atoms in PTFE has been investigated. PTFE was positioned downstream from the hydrogen plasma zone and was interacted predominantly with hydrogen radicals in the hydrogen plasma. We call this process remote plasma treatment to distinguish it from conventional plasma treatment. In conventional plasma treatment, PTFE is in the plasma zone and is interacted with all activated species such as electrons, ions, and radicals. This is an essential difference between remote and direct plasma treatments. We call the convention process direct plasma treatment in this paper. The surface of the PTFE treated by the remote plasma treatments has been investigated by means of contact angle measurement and XPS. The contribution of hydrogen radicals to the surface modification of PTFE has been discussed in comparison with that of plasma including electrons, ions, and radicals.

2. Theoretical Background of Remote Hydrogen Treatment

Remote hydrogen plasma treatment is expected to lead predominantly to interactions with hydrogen radicals rather than electrons and hydrogen ions, because the concentration of hydrogen radicals in a remote position from the plasma zone may be higher than that of electrons and hydrogen ions. Is this expectation true? Before performing the remote plasma treatment experiment, we ascertained whether the expectation is possible from simulation of the kinetics of hydrogen plasma.

Many investigators[8−12] simulated kinetics in plasmas such as hydrogen, oxygen, and silane plasma and showed a distribution of activated species in an after-

* To whom correspondence should be addressed.
[⊗] Abstract published in *Advance ACS Abstracts,* May 1, 1996.

S0024-9297(95)01072-2 CCC: $12.00

1. Generation of active species

					Rate Constant
$e + H_2 \xrightarrow{k_1}$	$H_2(v_1) + e$	(1)	$k_1 = 8.81 \times 10^{-10}$ cm^3/sec
$e + H_2 \xrightarrow{k_2}$	$H_2(v_2) + e$	(2)	$k_2 = 3.88 \times 10^{-11}$
$e + H_2 \xrightarrow{k_3}$	$H_2^* + e$	(3)	$k_3 = 1.28 \times 10^{-11}$
$e + H_2 \xrightarrow{k_4}$	$H_2^+ + 2e$	(4)	$k_4 = 2.32 \times 10^{-11}$
$e + H_2 \xrightarrow{k_5}$	$2H + e$	(5)	$k_5 = 4.49 \times 10^{-12}$
$e + H \xrightarrow{k_6}$	$H^* + e$	(6)	$k_6 = 9.90 \times 10^{-12}$
$e + H \xrightarrow{k_7}$	$H^+ + 2e$	(7)	$k_7 = 2.62 \times 10^{-13}$

2. Radiative decay of excimers

$H_2^* \xrightarrow{k_8}$	H_2	(8)	$k_8 = 1.00 \times 10^{7}$ l/sec
$H^* \xrightarrow{k_9}$	H	(9)	$k_9 = 2.00 \times 10^{7}$

3. Recombination between electron and hydrogen ion

$e + H_2^+ \xrightarrow{k_{10}}$	$H^* + H$	(10)	$k_{10} = 5.66 \times 10^{-8}$ cm^3/sec
$e + H^+ \xrightarrow{k_{11}}$	H^*	(11)	$k_{11} = 2.62 \times 10^{-13}$

4. Recombination between hydrogen radicals

$H + H + H_2 \xrightarrow{k_{12}}$	$H_2 + H_2$	(12)	$k_{12} = 8.3 \times 10^{-33}$ cm^6/sec
$H + H_{ad} \xrightarrow{k_{13}}$	H_2	(13)	

Figure 1. Elemental reactions in hydrogen plasma.

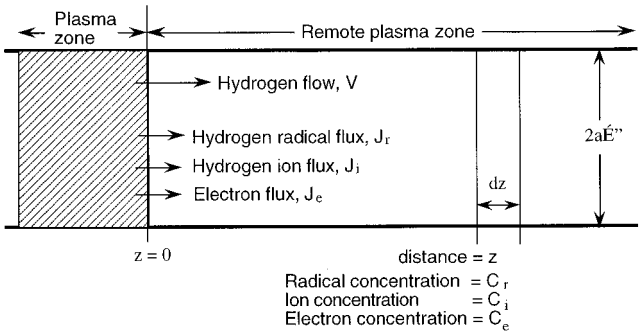

Figure 2. Model used for simulating the kinetics of the hydrogen plasma.

glow region. Their simulation did not deal with all activated species but with either radicals or electrons, and ions, although the plasma contains radicals, electrons, and ions. Radicals, electrons and ions inherently possess different behavior in chemistry and show different chemical reactions among them. Therefore, we believe that the simulation should deal with three species with essentially different chemical reactivities to understand the interactions between the polymer surface and the plasma. The simulation procedure used by an predecessors is helpful for us to simulate kinetics of all hydrogen radicals, electrons, and hydrogen ions.

Elemental reactions in hydrogen plasma are the generation of activated species by collision with electrons, radiative decay of the excimer, recombination between electron and ion, and recombination between two radicals. The activated species generated by the electron collision are hydrogen molecules with excited vibrational states ($H_2(v_1)$ and $H_2(v_2)$), excimer (H_2^* and H^*), hydrogen ions (H_2^+ and H^+), and hydrogen radicals (atoms) (H).[8] The details of these elemental reactions are shown in Figure 1.[8] A model as shown in Figure 2 is applied for simulating the remote hydrogen plasma: A cylindrical tube with a diameter of $2a$ cm and a length of L cm is connected at an end of the tube with the plasma zone. Hydrogen gas is flowed at a constant velocity of V cm/s in the direction from the plasma zone to the other end of the tube. The origin is the end of the plasma zone, and the position of z is defined as a distance of z cm from the origin in the direction of the hydrogen gas flow. We simulate concentrations of electrons (C_e), hydrogen ions (C_i), and hydrogen radicals (C_r) as a function of the distance z. In developing the model, we have the following assumptions:

(1) Activated species are generated in the plasma zone but never generated at $z > 0$.

(2) At a distance of $z > 0$, hydrogen radicals are drifted by the hydrogen flux and diffusion. Electrons and hydrogen ions are drifted by the hydrogen flux, diffusion, and electric field.

(3) The cylindrical tube is 4.5-cm diameter ($2a$) and 80 cm long (L). The hydrogen plasma is operated at an rf power of 50 W, at a hydrogen flow rate of 10 cm^3 (STP)/min (the velocity (V) corresponds to 9.6×10 cm/s at 330 K at 0.1 Torr), and at a pressure of 0.1 Torr. The temperature of the hydrogen flux is 330 K (57 °C). The electron temperature in the remote zone is 1 eV (11 600 K).

2.1. Concentration Distribution of Hydrogen Radicals. We consider the one-dimensional mass balance between a position of z and $z + dz$. The differential coefficient (dJ_r/dz) of the hydrogen radical flux (J_r) at a distance of z is equal to the generation rate of hydrogen radical (R_r) in a space of dz:

$$\frac{dJ_r}{dz} = R_r \tag{1}$$

The hydrogen radical flux (J_r) at z is given by the two modes of the radical drifting (hydrogen flux and diffusion):

$$J_r = C_r V - D_r \frac{dC_r}{dz} \tag{2}$$

where C_r, V, and D_r are the hydrogen radical concentration, the velocity of the hydrogen flow, and the diffusion coefficient of the hydrogen radicals, respectively, since in our condition the diffusion velocity ($>10^2$ cm/s) is greatly larger than the hydrogen flux (V) ($<10^2$ cm/s). Therefore, the hydrogen radical flux (J_r) is modified in eq 3.

$$J_r = -D_r \frac{dC_r}{dz} \tag{3}$$

From assumption 1, no hydrogen radical is generated at a space of dz, and the disappearance of hydrogen radicals (recombination of radicals) alone occurs. Therefore, the generation rate (R_r) of hydrogen radical is negative, and corresponds to the disappearance rate. There are two modes of the recombination reactions as shown in Figure 1: the three-body reaction (reaction 12) and the recombination at the surface of the tube wall (reaction 13). Wei and Phillips[10] said that the recombination at the wall surface (reaction 13) was insignificant relative to the three-body reaction (reaction 12), although reaction 13 occurred slightly. We believe that the three-body reaction may be a predominant recombination. The rate constant (k_{12}) of the three-body reaction is given by[12]

$$k_{12} = 2.7 \times 10^{-31} T^{-0.6} \quad \text{cm}^6\ \text{s}^{-1} \tag{4}$$

From eq 4, k_{12} at 330 K is estimated to be 8.3×10^{-33} cm^6 s^{-1}. Therefore, the disappearance rate (R_r) is

written as follows:

$$R_r = -k_{12}C_r \tag{5}$$

Combination of eqs 1, 3, and 5 leads to a differential equation with regard to the hydrogen radical concentration at z:

$$D_r \frac{d^2C_r}{dz^2} = k_{12}C_r \tag{6}$$

The D_r value at 330 K at 0.1 Torr is estimated to be 2.18×10^4 cm^2/s from the relationship $D_r = (AT^{1.5})/P$, where T (in K) and P (in Torr) are the temperature and pressure, respectively, and from the D_r data measured at a temperature range of 281−354 K at 760 Torr.[13−16] The solution of eq 6 is expressed as follows:

$$C_r = C_r^0 \exp[-(k_{12}/D_r)^{1/2}z] \tag{7}$$

$$k_{12} = 8.3 \times 10^{-33} \qquad D_r = 2.18 \times 10^4$$

$$(k_{12}/D_r)^{1/2} = 6.2 \times 10^{-19}$$

where C_r^0 is the hydrogen radical concentration at $z = 0$.

2.2. Concentration Distribution of Electrons and Hydrogen Ions. We consider a similar one-dimensional mass balance between a distance of z and $z + dz$ with regard to the electron flux (J_e) and hydrogen ion flux (J_i). The simulation procedure is the same as that used for the simulation of the radical concentration.

$$\frac{dJ_e}{dz} = R_e \tag{8}$$

$$\frac{dJ_i}{dz} = R_i \tag{9}$$

The electron flux (J_e) and hydrogen ion flux (J_i) are written by the three drafting modes (hydrogen flux, diffusion, and electric field):

$$J_e = C_eV - D_e\frac{dC_e}{dz} - C_e\mu_eE \tag{10}$$

$$J_i = C_iV - D_i\frac{dC_i}{dz} + C_i\mu_iE \tag{11}$$

where C_e and C_i are the electron and hydrogen ion concentrations at z, respectively. D_e and D_i are the diffusion coefficients of the electron and the hydrogen ion, respectively. μ_e and μ_i are the mobilities driven by the electric field for the electron and the hydrogen ion, respectively. From neutrality, $J_e = J_i$ and $C_e = C_i$, the combination of eqs 10 and 11 leads to

$$C_cV - D_e\frac{dC_c}{dz} - C_e\mu_eE = C_cV - D_i\frac{dC_c}{dz} + C_i\mu_iE \tag{12}$$

In the case of $C_c = C_e = C_i$, eq 12 is reduced to

$$C_c(\mu_i + \mu_e)E = (D_i - D_e)\frac{dC_c}{dz}$$

$$E = \frac{D_i - D_e}{\mu_i + \mu_e}\frac{1}{C_c}\frac{dC_c}{dz} \tag{13}$$

Therefore, the combination of eqs 10, 11, and 13 leads to the following equation:

$$J_c = J_e = J_i = C_cV - \frac{D_i - D_e}{\mu_i + \mu_e}\frac{1}{C_c}\frac{dC_c}{dz} \tag{14}$$

From the assumption that no electron and hydrogen ion are generated in a space of dz and the disappearance alone occurs, the generation rates of the electron (R_e) and hydrogen ion (R_i) are negative and are written as follows:

$$R_c = R_e = R_i = -(k_{10} + k_{11})C_eC_i = -(k_{10} + k_{11})C_c^2 \tag{15}$$

Therefore, the combination of eqs 8, 9, 14, and 15 leads to

$$\frac{d}{dz}\left\{C_cV - \frac{\mu_eD_i + \mu_iD_e}{\mu_i + \mu_e}\frac{dC_c}{dz}\right\} = -(k_{10} + k_{11})C_c^2 \tag{16}$$

Since the diffusion velocity (>10^2 cm/s) in our case is much higher than the hydrogen flow velocity (V) (<10^2 cm/s), eq 16 is reduced to

$$\frac{\mu_eD_i + \mu_iD_e}{\mu_i + \mu_e}\frac{d^2C_c}{dz^2} = (k_{10} + k_{11})C_c^2 \tag{17}$$

The mobilities of the electron and the ion (μ_e and μ_i) are related to the diffusion coefficient and the electron and ion temperatures:[10]

$$\frac{D_e}{\mu_e} = \frac{k}{e}T_e \tag{18}$$

$$\frac{D_i}{\mu_i} = \frac{k}{e}T_i \tag{19}$$

where k and e are Boltzman's constant and the charge of the electron. Under the assumption that the ion temperature is almost equal to the hydrogen gas temperature ($T_g = 330$ K), eq 19 is modified as follows:

$$\frac{D_i}{\mu_i} = \frac{k}{e}T_g \tag{20}$$

The combination of eqs 18−20 leads to

$$\frac{\mu_iD_e + \mu_eD_i}{\mu_i + \mu_e} = \frac{\mu_i}{\mu_e}D_e + D_i = (T_e + T_g)\frac{k}{e}\mu_i \tag{21}$$

The mobility (μ_i) of the hydrogen ion is expressed as a function of T_g (in K) and P (in Torr).[10,17]

$$\mu_i = \mu_i^0\frac{760}{P}\frac{T_g}{273.16} \tag{22}$$

where μ_i^0 is the mobility of hydrogen ion at 273.16 K at 760 Torr. Since the mobilities for H^+ and H_2^+ ions are 11.2×10^3 and 10×10^3 cm^2/s at 273 K at 1 Torr, respectively,[18] the mobility of the hydrogen ions (H^+ and H_2^+) at 330 K at 0.1 Torr is estimated to be about 1.3×10^5 cm^2/s. Therefore,

$$\frac{\mu_iD_e + \mu_eD_i}{\mu_i + \mu_e} = (T_e + T_i)\frac{k}{e}\mu_i = 1.3 \times 10^5 \text{ cm}^2/\text{s}$$

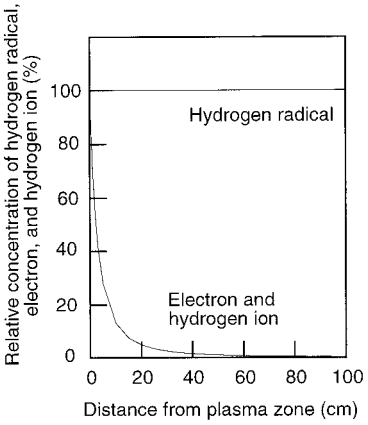

Figure 3. Relative concentration of the hydrogen radicals (C_r/C_r^0), and electron and hydrogen ions (C_c/C_c^0) as a function of distance from the plasma zone.

Finally, the solution of eq 17 is expressed as follows:

$$C_c = \frac{C_c^0}{\left[1 + \left(\frac{C_c^0(k_{10} + k_{11})}{6[(\mu_i D_e + \mu_e D_i)/(\mu_i + \mu_e)]}\right)^{1/2} z\right]^2} \quad (23)$$

$$\frac{\mu_i D_e + \mu_e D_i}{\mu_i + \mu_e} = 1.3 \times 10^5 \qquad k_{10} + k_{11} = 5.66 \times 10^{-8}$$

$$\left[\frac{k_{10} + k_{11}}{6[(\mu_i D_e + \mu_e D_i)/(\mu_i + \mu_e)]}\right]^{1/2} = 2.7 \times 10^{-7}$$

where C_c^0 is the electron and hydrogen concentrations at $z = 0$ cm.

2.3. Comparison between the Hydrogen Radical Concentration and the Electron or Hydrogen Ion Concentration in the Remote Plasma Zone. The simulation of kinetics in hydrogen plasma, as described in section 2.1 and 2.2, shows that the hydrogen radical concentration, C_r, is expressed by an exponential formula as a function of z (eq 7), and the electron and hydrogen ion concentrations, C_c, are expressed by a complicated function of z (eq 23). Using the Mathematica program (Wolfram Research Inc., ver. 2.2), numerical calculation of eqs 7 and 23 was done. Figure 3 shows the relative concentration of the hydrogen radical (C_r/C_r^0) and of the electron and hydrogen ion (C_c/C_c^0) as a function of the distance (z) from the end of the plasma zone. The concentration (C_r/C_r^0) of the hydrogen radical, as shown in Figure 3, shows a negligible decrease with increasing the distance of z up to a distance of 100 cm. At $z = 50$ and 80 cm, the relative concentration is about 100%. On the other hand, the electron and hydrogen concentration (C_c/C_c^0) shows a rapid decrease with increasing the distance of z, and the relative concentrations (C_c/C_c^0) at $z = 50$ and 80 cm reach about 10% and less than 1%, respectively. This comparison shows that as the distance (z) increases, the action of the hydrogen radicals may become predominant relative to that of the electrons and hydrogen ions. Conclusively, the simulation of the kinetics of the hydrogen plasma ascertains a possibility that interaction reactions with hydrogen radicals rather than electrons and hydrogen ions occur predominantly in the remote hydrogen plasma.

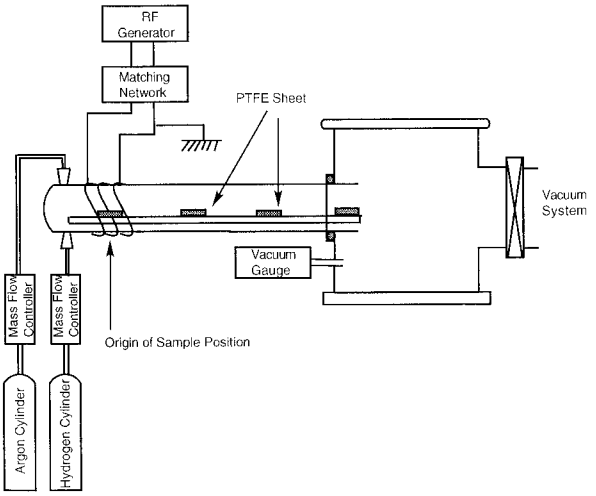

Figure 4. Schematic representation of the remote plasma reactor.

3. Experimental Section

3.1. Materials. The poly(tetrafluoroethylene), PTFE, sheet, which was received from Nitto Denko Co. (Nitofuron NO900UL) as 300 mm wide and 1 μm thick, was cut to a dimension of 10 mm x 30 mm, and was provided as a specimen for surface modification experiments. Prior to the experiment, the sheet was washed with acetone in an ultrasonic washer and dried at room temperature under vacuum. Argon and hydrogen were pure grade, and the purity was 99.995%.

3.2. Plasma Reactor for Remote Hydrogen Plasma Treatment. A special reactor for the remote hydrogen plasma treatment of the PTFE sheet was used. The reactor consisted of a cylindrical Pyrex glass tube (45 mm diameter, 1000 mm long) and a columnar stainless steel chamber (300 mm diameter, 300 mm height). The Pyrex glass tube had two gas inlets for the injection of hydrogen and argon gases and a copper coil of nine turns for the energy input of rf power (13.56 MHz frequency). The gas inlets and the copper coil was attached to the Pyrex glass tube at a distances of 50 and 200 mm from the glass tube end, respectively. The stainless steel chamber contained a Barocel pressure sensor (Type 622, Edwards) and a vacuum system of a combination of a rotary pump (320 L/min) and a diffusion pump (550 L/sec) (Type YH-350A, Ulvac Co.). The Pyrex glass tube was jointed with the chamber in a manner of Viton O ring flange. The schematic diagram of the reactor is shown in Figure 4.

3.3. Remote Hydrogen Plasma Treatment. To assess the modification by the hydrogen plasma as a function of the sample position, the PTFE sheets were positioned at a constant distance of 0, 250, 500, 750, and 800 mm from the center of the copper coil and were exposed to the hydrogen plasma. In the concrete, the PTFE sheets were mounted at given positions on a glass plate (400 mm wide, 1000 mm long) with double-sided adhesive tape, and the glass plate was set up in the Pyrex glass tube of the reactor. First, air in the reaction system was displaced with argon. Afterward, the reaction chamber was evacuated to approximately 1.3×10^{-2} Pa, and then hydrogen whose flow rate was adjusted to 10 cm^3 (STP)/min by a mass flow controller was introduced into the Pyrex glass tube. The hydrogen plasma was operated at an rf power of 25, 50, 75, and 100 W at 13.56-MHz frequency at a system pressure of 13.3 Pa.

3.4. Advancing Contact Angle of Water. The advancing contact angles of water on the PTFE sheet surfaces treated with the hydrogen plasma were measured at 20 °C using an Erma contact angle meter with a goniometer (Model G-1). Twice-distilled water was used for the contact angle measurement. A drop (1 μL) of the water was transferred to the plasma-treated PTFE surface, and the height (h) and the width (w) of the drop on the PTFE surface were measured using a telescope with a scale. The advancing contact angle (θ) of the drop was estimated from the equation $\theta/2 = \tan^{-1}(2h/w)$. The

advancing contact angle determined was an average of 10 measurements. A standard deviation of the 10 measurements was within 1°.

3.5. X-ray Photoelectron Spectra. The XPS spectra of the surface of the PTFE sheets treated with the remote hydrogen plasma were obtained on a Shimadzu ESCA K1 using a nonmonochromatic Mg Kα photon source. The anode voltage was 10 kV, the anode current 30 mA, and the background pressure in the analytical chamber 1.5×10^{-6} Pa. The size of the X ray spot was 2-mm diameters and the take-off angle of photoelectrons was 90° with respect to the sample surface. The XPS spectra were referenced with respect to the 690.0 eV fluorine 1s core level to eliminate the charge effect. The smoothing procedure of the spectra was not done. The C_{1s} and O_{1s} spectra were decomposed by fitting a Gaussian−Lorentzian mixture function (the mixture ratio was 80:20) to an experimental curve using a nonlinear, least-squares curve-fitting program, ESCAPAC, supplied by Shimadzu. The sensitivity factors (S) for the core levels were $S(C_{1s}) = 1.00$, $S(O_{1s}) = 2.85$, and $S(F_{1s}) = 4.26$. The experimental errors for estimating the F/C and O/C atomic ratios from the relative F_{1s}, O_{1s}, and C_{1s} intensities were ±0.01.

Angular XPS spectra of the PTFE sheets treated with the remote hydrogen plasma were obtained at take-off angles of 45° (sin $\theta = 0.707$), 33.4° (sin $\theta = 0.550$), 20.5° (sin $\theta = 0.350$), and 14.5° (sin $\theta = 0.250$) with respect to the sample surface on an ULVAC PHI ESCA system 5500 using a nonmonochromatic Mg Kα photon source. The anode power was 300 W, the background pressure in the analytical chamber was 3.3×10^{-7} Pa, and the size of the X ray spot was 7 mm diameter.

4. Results and Discussion

4.1. Advancing Contact Angle of Water on the Hydrogen Plasma-Treated PTFE Sheet. The hydrogen plasma emitted a purplish red glow, and the glow was expanded to the downstream direction by increasing the rf power. We observed with our naked eye that the glow in the Pyrex glass tube of the reactor was in a space within 50 cm from the center of the rf coil, even when an rf power level of 100 W was applied. The relative composition of electrons, hydrogen ions, and hydrogen radicals (hydrogen atoms), as described in section 2, is related to the position in the Pyrex glass tube as well as to the rf power. Therefore, surface modification of the PTFE sheets by the hydrogen plasma was investigated as functions of the sample position as well as the rf power and the plasma exposure time.

The PTFE sheets were set-up at sample positions of 0, 25, 50, 75, and 80 cm from the center of the rf coil in the Pyrex glass tube of the reactor and were exposed to the hydrogen plasma at rf power levels of 25, 50, 75, and 100 W. The modification of the PTFE sheet by the hydrogen plasma was investigated from the advancing contact angle of water on the surface of the treated PTFE sheets as a function of the plasma exposure time, the rf power, and the sample position. The contact angle measurements were carried out immediately after finishing the plasma exposure experiments to minimize changes in the surface properties. Regardless of the treatment conditions (the plasma exposure time, the rf power, and the sample position), the PTFE sheets treated with the hydrogen plasma (89−67°) showed smaller advancing contact angles than the original PTFE sheet (120°), and their surfaces became hydrophilic. The hydrophilicity showed a strong dependence on the plasma exposure time, the rf power, and the sample position. Figures 5, 6 and 7 show typical effects of the plasma exposure time, the rf power, and the sample position on the hydrophilicity. In these figures, the hydrophilicity is evaluated by the cosine of the advancing contact angle (θ), cos θ. The plasma exposure

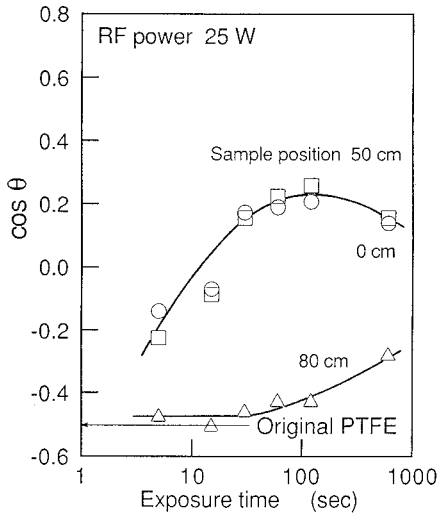

Figure 5. Advancing contact angle of water at the surface of hydrogen-plasma-treated PTFE sheets as functions of plasma exposure time and sample position (rf power of 25 W): sample positions of (○) 0 cm; (□) 50 cm, and (△) 80 cm.

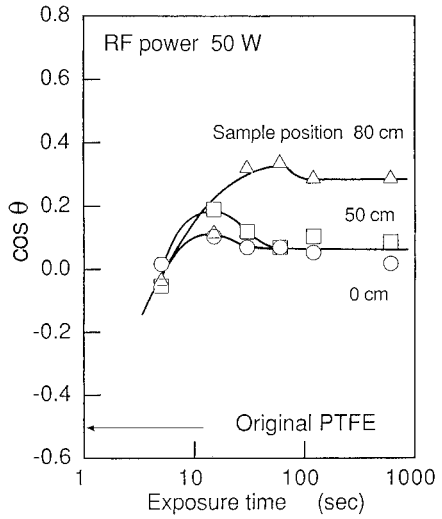

Figure 6. Advancing contact angle of water at the surface of hydrogen-plasma-treated PTFE sheets as functions of plasma exposure time and sample position (rf power of 50 W): sample positions of (○) 0 cm, (□) 50 cm, (△) 80 cm.

time shows two types of effects: One is no effect of the plasma exposure time on cos θ. The effect appears at sample positions 0−25 cm from the center of the copper coil regardless of the rf power, except 25 W. cos θ is a constant of 0.02−0.07 (θ = 89−86°) for an rf power of 50 W and of 0.04−0.09 (θ = 88−85°) for rf powers of 75 and 100 W. The other is a strong effect of the plasma exposure time on cos θ. This effect appears at sample positions far from the plasma zone, especially at a sample position of 80 cm. cos θ, as shown in Figures 6 and 7, increases by increasing the plasma exposure time and is maximized at an exposure time of about 120 s. cos θ at the maximum is higher than that at a sample position of 0 cm. The effects of the rf power were also observed: For example, cos θ for the PTFE sheets modified at rf powers of 25, 50, and 75 W is −0.42 (θ = 115°), 0.29 (θ = 73°), and 0.55 (θ = 57°), respectively. The sample position effect is distinguished from the plasma exposure time and rf power effects. Figure 8 shows cos θ for the PTFE sheet modified with the hydrogen plasma for 120 s as a function of the sample position. cos θ at sample positions of 0−50 cm, as shown in Figure 5, is almost constant (cos θ is 0.22−0.26 for

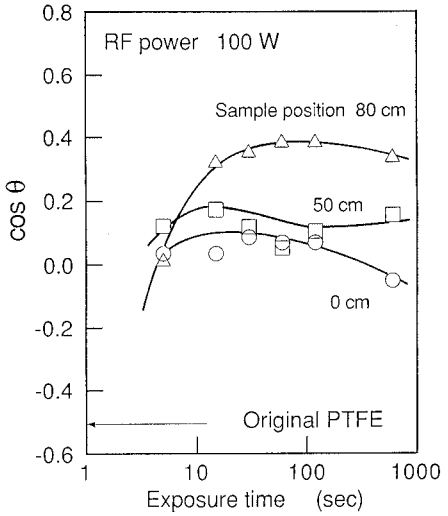

Figure 7. Advancing contact angle of water at the surface of hydrogen-plasma-treated PTFE sheets as functions of plasma exposure time and sample position (rf power of 100 W): sample positions of (○) 0 cm, (□) 50 cm, and (△) 80 cm.

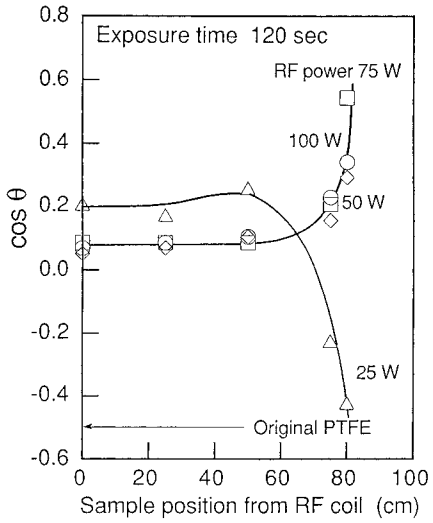

Figure 8. Advancing contact angle of water at the surface of hydrogen-plasma-treated PTFE sheets as functions of rf power and sample position (plasma exposure time of 120 s: rf power of (△) 25 W, (◇) 50 W, (□) 75 W, and (○) 100 W.

an rf power of 25 W and 0.08−0.10 for 50, 75, and 100 W). On the other hand, cos θ at sample positions of more than 75 cm, except that for the PTFE sheet treated at an rf power of 25 W, rises up rapidly by increasing the sample position. cos θ at a sample position of 80 cm reaches 0.29 for 50 W, 0.55 for 75 W, and 0.39 for 100 W. These values are fairly higher than that at 0 cm, indicating that the hydrogen plasma exposure at a sample position of 80 cm is a better way for hydrophilic modification than that at a sample position of 0 cm. Here we call the hydrogen plasma treatment at a sample position of 80 cm the remote hydrogen plasma treatment to distinguish it from conventional hydrogen plasma treatment, which is done at a sample position of 0 cm. We also call conventional hydrogen plasma treatment direct hydrogen plasma treatment.

From these results, we conclude the following: (1) The hydrogen plasma makes the surface of the PTFE sheet hydrophilic. (2) The hydrophilicity depends on the sample position as well as the rf power and the plasma exposure time. The sample position influences the hydrophilicity. (3) Remote hydrogen plasma exposure (at a sample position of 80 cm) leads to higher hydrophilicity than direct hydrogen plasma exposure (at a sample position of 0 cm). In the next section, we will discuss the question, "is there any difference in the chemical composition between the surfaces of the PTFE sheets treated with the remote and direct hydrogen plasmas?"

Table 1. Atomic Composition of Remote and Direct Hydrogen-Plasma-Treated PTFE Sheets

surface modification			atomic comp	
plasma	rf power, W	exposure time, s	F/C	O/C
nonr			1.92	0.05
remote	75	120	0.41	0.12
direct	75	120	0.60	0.07

4.2. Chemical Composition of the Surface of the PTFE Sheet Treated with Remote and Direct Hydrogen Plasmas. The atomic composition at the surface of the PTFE sheets treated with the remote and direct hydrogen plasmas was analyzed by XPS. The specimens for the analysis were the PTFE sheets which were set-up at sample positions of 0 and 80 cm from the center of the rf coil and treated with the hydrogen plasma at 75 W for 120 s. Table 1 shows the atomic composition (F/C and O/C atom ratio) for the PTFE sheets treated with the remote and direct hydrogen plasmas. The atomic composition was determined from XPS analysis. The PTFE sheets treated with both remote and direct hydrogen plasmas, as shown in Table 1, show some decreases in the F/C atom ratio (the F/C atom ratio is 0.41 and 0.60, respectively.) compared with the original PTFE sheet (the F/C atom ratio is 1.92). It is obvious that the remote and direct hydrogen plasma treatments initiated the defluorination of the PTFE sheet. The remote hydrogen plasma treatment gives a lower F/C atom ratio (F/C = 0.41) than the direct hydrogen plasma treatment (F/C = 0.60). This indicates that the remote hydrogen plasma contributes more effectively to the defluorination from the PTFE sheet than the direct hydrogen plasma.

The PTFE sheets treated with both remote and direct hydrogen plasmas also contain small amounts of oxygen moieties. Although the original PTFE sheet already contains oxygen moieties (the O/C atom ratio is 0.05) before the plasma treatments, the hydrogen-plasma-treated PTFE sheets and, especially, the remote hydrogen-plasma-treated sheet contain a larger amount of oxygen moieties: The O/C atom ratio for the remote and direct hydrogen-plasma-treated PTFE sheets is 0.12 and 0.07, respectively. The generation of the oxygen moieties may be due to postreactions of carbon radicals with oxygen in air after the plasma treatment. Carbon radicals are formed by means of abstraction reactions of fluorine atoms from the PTFE surface by hydrogen atoms and by means of the bond scission of the C−F and C−C bonds by electron and ion bombardment. We do not interpret why the concentration of the oxygen moieties is higher for the remote hydrogen-plasma-treated PTFE sheet than for the direct hydrogen-plasma-treated PTFE sheet.

Conclusively, the main reaction initiated by both remote and direct hydrogen plasmas is the defluorination reaction of the PTFE sheet surface. The remote hydrogen plasma has a higher capability for defluorination than the direct hydrogen plasma.

XPS spectra, especially the C_{1s} spectra, gave useful information on the chemical composition of the PTFE sheets treated with both remote and direct hydrogen plasmas. In this section, the chemical compositions of

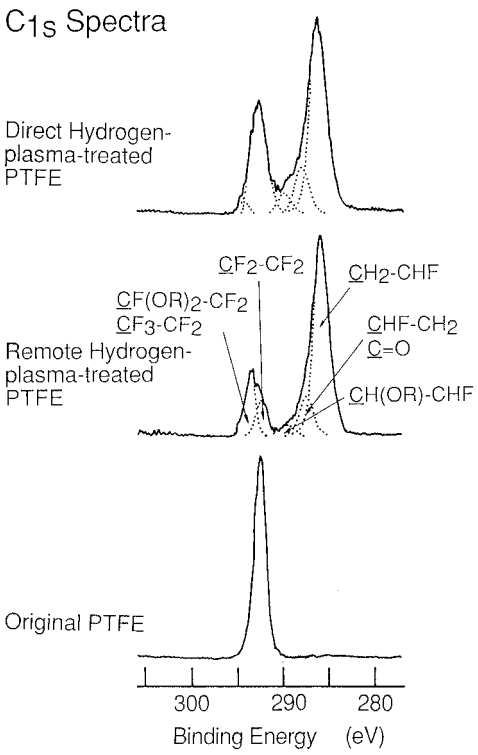

Figure 9. C_{1s} spectra of remote and direct hydrogen-plasma-treated PTFE sheets at an rf power of 75 W for 120 s.

the PTFE sheets treated with the remote and direct hydrogen plasmas are discussed from the viewpoint of the XPS spectra. The specimens for XPS measurement are typical PTFE sheets which were treated at the sample positions of 80 cm (remote plasma treatment) and 0 cm (direct plasma treatment) with the hydrogen plasma at 75 W for 120 s. The two sheets have high hydrophilic surfaces: cos θ is 0.55 for the remote hydrogen-plasma-treated PTFE sheet and 0.09 for the direct hydrogen-plasma-treated PTFE sheet.

Figure 9 compares the C_{1s} spectra of the original PTFE sheet and the two PTFE sheets treated with the remote and direct hydrogen plasmas at an rf power of 75 W for 120 s. The C_{1s} spectra give important information with respect to the chemistry of the fluorinated carbon atoms, because of a large chemical shift of fluorine atom.[19] The result of the decomposition is illustrated in dotted lines in each of the spectra in Figure 9. The original PTFE sheet, as shown in Figure 9, shows a symmetrical spectrum appearing at 292.5 eV due to the CF_2-CF_2 unit. The full width at half-maximum (FWHM) value of the spectrum is 1.5 eV. Both remote and direct hydrogen-plasma-treated PTFE sheets, as shown in Figure 9, show complex C_{1s} spectra having two peaks. These spectra are decomposed into five components appearing at 285.9−296.0, 287.6−287.9, 289.6−289.8, 292.5, and 293.7−294.1 eV. From the reference of the primary and secondary chemical shifts of the fluorine and oxygen atoms,[19,20] these five components can be assigned to the *C*H_2CHF groups (at 285.9−296.0 eV), *C*HFCH_2 and C=O groups (at 287.6−287.9 eV), *C*H(OR)CHF groups (at 289.6−289.8 eV), *C*F_2CF_2 groups (at 292.5 eV), and *C*F_3CF_2 and/or *C*F$(OR)_2$CF_2 groups (at 293.7−294.1 eV). The underlined carbon atom is the objective carbon atom for the assignment. The fifth component at 293.7−294.1 eV is assigned to a mixture of the *C*F_3CF_2 and *C*F$(OR)_2$CF_2 groups, or of either the *C*F_3CF_2 groups or the *C*F$(OR)_2$-CF_2 groups. The assignment of the *C*F(OR)CF_2 groups rather than the *C*F_3CF_2 groups may be reasonable, because the O/C atom ratio in the plasma-treated-PTFE sheets (the O/C atom ratio is 0.12 for the remote hydrogen-plasma-treated PTFE sheet and 0.07 for the direct hydrogen-plasma-treated PTFE sheet) corresponds to the sum of the concentration of the *C*F-$(OR)_2$CF_2 and *C*H(OR)CHF groups (16% of the total carbon atoms for the remote hydrogen-plasma-treated PTFE sheet and 7% for the direct hydrogen-plasma-treated PTFE sheet). However, the determination never excluded the assignment of the *C*F_3CF_2 groups.

These spectra show that both remote and direct hydrogen plasmas make up the substitution of the hydrogen atom for the fluorine atom of the PTFE surface to form the CHF and CH_2 units. The relative concentrations of the five components are estimated from the relative peak areas of the decompositions (Table 2). Table 2 shows that the main product is the dihydrogen-substituted carbon atom (CH_2 groups), which accounts for 63% of the total carbon atoms for the remote hydrogen-plasma treated PTFE sheet and for 55% for the direct hydrogen-plasma-treated PTFE sheet. The monohydrogen-substituted carbon atom (CHF groups) is 12% for the two plasma-treated PTFE sheets. The unsubstituted carbon atom (CF_2 groups) is only 9% and 26% for the remote and direct hydrogen-plasma treated PTFE sheets, respectively. Therefore, the reactivities of the CF_2 groups are 91% and 74% for the remote and direct hydrogen plasma treatments, respectively. This indicates that the remote hydrogen plasma has a higher capability of the substitution than direct hydrogen plasma.

The original PTFE sheet, as shown in Figure 10, shows a poor O_{1s} spectrum because of low oxygen concentration, and the signal/noise ratio is not high enough for the decomposition process. The remote and direct hydrogen-plasma-treated PTFE sheets showed good O_{1s} spectra for the decomposition. The spectra, as illustrated by dotted lines in Figure 10, are decomposed into two components, which appear at 532.3−532.4 and 533.6−533.7 eV. The first component at 532.3−532.4 eV is assigned the O=C groups, and the other is assigned to the OC groups.[19] The relative compositions of the O=C and OC groups are 73−74% and 26−27%, respectively (Table 2). There is no difference in the relative composition of the oxygen groups between the remote and direct hydrogen-plasma-treated PTFE sheets, although there is about two times the difference in the oxygen atom concentration between the remote and direct hydrogen-plasma-treated PTFE sheets. This similarity in relative compositions of the O=C and OC groups between the remote and direct hydrogen-plasma-

Table 2. Chemical Composition of Remote and Direct Hydrogen-Plasma-Treated PTFE Sheets

surface modification			C_{1s} component, %					O_{1s} component, %	
plasma	rf power, W	exposure time, s	*C*H_2CHF	*C*HFCH_2 and C=O	*C*H(OR)CHF	*C*F_2CF_2	*C*F$(OR)_2$CF_2 and *C*F_3CF_2	O=C	OC
none			0	0	0	100	0		
remote	75	120	63	12	3	9	13	27	73
direct	75	120	55	12	5	26	2	26	74

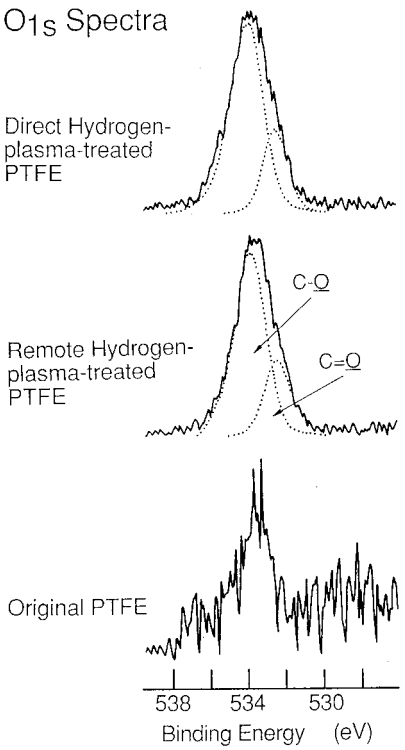

Figure 10. O_{1s} spectra of remote and direct hydrogen-plasma-treated PTFE sheets at an rf power of 75 W for 120 s.

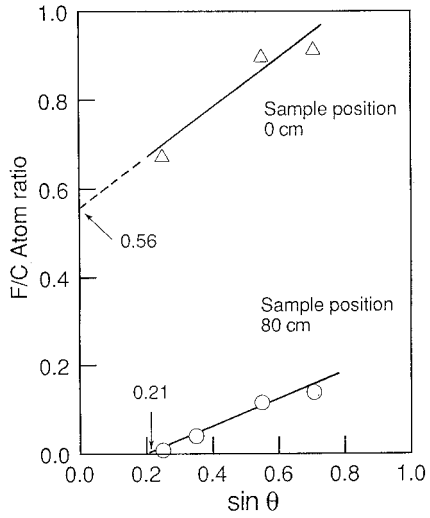

Figure 11. Depth profile of F/C atom ratio for remote and direct hydrogen-plasma-treated PTFE sheets at an rf power of 75 W for 120 s as a function of the take-off angle.

treated PTFE sheets may be a natural consequence because the formation of these oxygen groups is due to the postreaction of carbon radicals with oxygen in air after finishing the hydrogen plasma treatment. Therefore, the oxidation process is free from how the carbon radicals are formed, once carbon radicals are formed.

From the results of the XPS spectra, we conclude that the remote and direct hydrogen plasmas lead to the substitution of hydrogen atoms for fluorine atoms in the PTFE sheet. The remote hydrogen plasma is more effective in the substitution than the direct hydrogen plasma. The main product of the substitution is the dihydrogen-substituted carbon unit, and reaches 63% and 55% of the total carbon atoms by the remote and direct hydrogen plasma treatments, respectively.

4.3. Depth Profile of the Surface of the PTFE Sheets treated with Remote and Direct Hydrogen Plasmas. The angular XPS measurement gives information with regard to the depth profile of the hydrogen substitution in the PTFE sheet by the remote and direct hydrogen plasmas. The specimens for the angular XPS measurement were the PTFE sheets treated with the remote and direct hydrogen plasmas at an rf power of 75 W for 120 s. Figures 11 and 12 show the F/C and O/C atom ratio for the remote and direct hydrogen-plasma-treated PTFE sheets, respectively, as a function of sin θ. θ is the take-off angle of photoelectrons with respect to the sample surface, and three or four take-off angles of 45 to 14.5° were chosen for the angular XPS spectra. When the PTFE surface is smooth, the sampling depth (d) is proportional to sin θ,

$$d = 3\lambda \sin\theta \tag{24}$$

where λ is the mean-free path of the photoelectrons. The mean-free path (λ in nm) is related to the kinetic energy of the photoelectrons (E in eV) and the density of the polymer (ρ in kg/m^3):[21]

$$\lambda = \frac{49}{10^{-3}\rho E^2} + \frac{0.11E^{0.5}}{10^{-3}\rho} \tag{25}$$

When ρ for the PTFE sheet is 2.18×10^3 kg/m^3 and E is 950−970 eV, λ is estimated from the eq 25 to be about 1.6 nm. Therefore, the sampling depth is calculated from the eq 24 to be about 1.2 and 3.4 nm at take-off angles of 14.5° and 45°, respectively. The F/C atom ratio for both hydrogen-plasma-treated PTFE sheets decreases linearly increasing the sampling depth (Figure 11), and the O/C atom ratio increases linearly (Figure 12). If the linear relationship can extend to the film surface, the F/C and O/C atom ratios at the surface of the hydrogen-plasma-treated PTFE sheets are estimated from the following extrapolation: For the remote hydrogen-plasma-treated PTFE sheet, the F/C and O/C atom ratios are 0 and 0.74, respectively, and for the direct hydrogen-plasma-treated PTFE sheet, the F/C and O/C atom ratios are 0.56 and 0.34, respectively. This figure shows that the substitution of hydrogen atoms for fluorine atoms in the PTFE sheet proceeded at least 3.4 nm from the topmost layer of the sheet. Especially in the remote hydrogen plasma treatment, the F/C atom ratio at the PTFE sheet surface is 0, and the complete

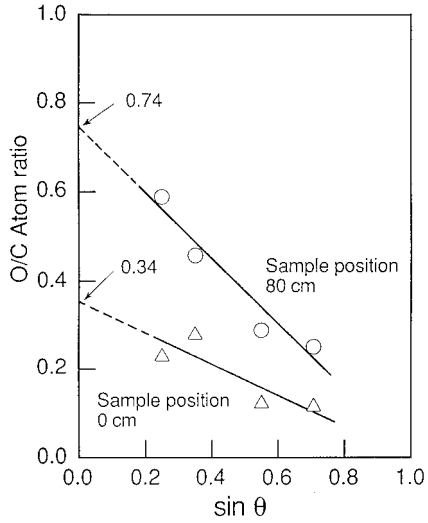

Figure 12. Depth profile of O/C atom ratio for remote and direct hydrogen-plasma-treated PTFE sheets at an rf power of 75 W for 120 s as a function of the take-off angle.

substitution occurred. This complete substitution proceeds not only at the sheet surface but also about 1 nm from the surface. From this comparison, we conclude that the remote hydrogen plasma is a more powerful agent in the hydrogen substitution of fluorine atoms in the PTFE sheet than the direct hydrogen plasma.

5. Conclusion

The kinetics of hydrogen plasma in an afterglow was simulated to distinguish remote plasma treatment from conventional (direct) plasma treatment. Experimentally, hydrogen substitution processes of the PTFE sheet by the remote and direct hydrogen plasma treatments have been investigated by means of contact angle measurement and XPS to ascertain the expectation from the simulation. Experimental results showed the accuracy of the simulation regarding the kinetics of the remote hydrogen plasma. The results are summarized as follows:

1. The simulation shows a possibility that the remote hydrogen plasma treatment can enhance interaction reactions with hydrogen radicals relative to those with electrons and hydrogen ions.

2. Both remote and direct hydrogen plasmas make the surface of the PTFE sheet hydrophilic. The hydrophilicity depends on the sample position as well as the rf power and the plasma exposure time. The sample position give a strong effect on the hydrophilicity. The remote hydrogen plasma leads to higher hydrophilicity than the direct hydrogen plasma.

3. The F/C atom ratio is 0.41 for the remote hydrogen-plasma-treated PTFE sheet, and 0.60 for the direct hydrogen-plasma-treated. The remote hydrogen plasma is more effective in defluorination than the direct hydrogen plasma. The main product is the dihydrogen-substituted carbon unit, and the concentration reaches 63% and 55% of the total carbon atoms by the remote and direct hydrogen plasma treatments, respectively.

4. The hydrogen substitution proceeds at least 3.4 nm from the surface of the PTFE sheet. The remote hydrogen plasma treatment especially accomplishes the complete substitution (the F/C atom ratio is 0). This complete substitution proceeds not only at the sheet surface but also at about 2 nm from the PTFE surface.

Acknowledgment. We acknowledge Professor M. Kando, Shizuoka University, for useful suggestions regarding the simulation of plasma kinetics. This work was supported by the Grant-in-Aid for Scientific Research Administered by the Ministry of Education, Science, and Culture, Japan.

References and Notes

(1) Satokawa, T. *Functional Fluoropolymers*; Nikkan Kogyo Shinbunsha: Tokyo, 1982.
(2) Hansen, R. H.; Schonhorn, H. *J. Polym. Sci., Polym. Lett. Ed.* **1966**, *4*, 203.
(3) Hollahan, J. R.; Stafford, B. B.; Falls, R. D.; Payn, S. T. *J. Appl. Polym. Sci.* **1969**, *13*, 807.
(4) Nakayama, Y.; Takahagi, T.; Soeda, F. *J. Polym. Sci., Polym. Chem. Ed.* **1988**, *26*, 559.
(5) Clark, D. T.; Hutton, D. R. *J. Polym. Sci., Polym. Chem. Ed.* **1987**, *25*, 2643.
(6) Inagaki, N.; Tasaka, S.; Kawai, H. *J. Adhesion Sci. Technol.* **1989**, *3*, 637.
(7) Goldman, A.; Amouroux, J. In *Electrical Breakdown and Discharge in Gases, Macroscopic Processess and Discharges*; Kunhardt, E. E., Luessen, L. H., Eds.; Plenum: New York, 1983; p 293.
(8) Kushner, M. J. *J. Appl. Phys.* **1988**, *63*, 2532.
(9) Chou, C.-H.; Wei, T.-C.; Phillips, *J. J. Appl. Phys.* **1992**, *72*, 870.
(10) Wei, T.-C; Phillips, T.-C. *J. Appl. Phys.* **1993**, *74*, 825.
(11) Rau, H.; Phicht, F. *J. Phys. D: Appl. Phys.* **1993**, *26*, 1260.
(12) Deson, J.; Halous, F.; Lalo, C; Rousseau, C.; Veniard, V. *J. Phys. D: Appl. Phys.* **1994**, *27*, 2320.
(13) Wise, H. *J. Chem. Phys.* **1961**, *34*, 2139.
(14) Weissman, S.; Mason, E. *J. Chem. Phys.* **1962**, *36*, 794.
(15) Knouw, B.; Morgan, J. E.; Schiff, H. I. *J. Chem. Phys.* **1969**, *50*, 66.
(16) Sancier, K. M.; Wise, H. *J. Chem. Phys.* **1969**, *51*, 1434.
(17) Morseley, I. T.; Snuggs, R. M.; Martin, D. W.; McDaniel, E. W. *Phys. Rev.* **1968**, *178*, 240.
(18) Hatta, Y. *Gas Discharge*; Kindai Kagaku-sha: Tokyo, **1968**; p 87.
(19) Beamson, G; Briggs, D. *High Resoution XPS of Organic Polymers*; Wiley: New York, 1992.
(20) Iwata, H.; Matsuda, T. In *Polymer Surface and its Applications*; Ikada, Y., Ed.; Kagaku Dojin: Kyoto, 1986; p78.
(21) Robert, R. F.; Allara, D. L.; Pryde, C. A.; Buchanan, D. N. E.; Hobbins, N. D. *Surf. Interface Anal.* **1980**, *2*, 5.

MA951072R